

The influence of inorganic materials on the pyrolysis of polytetrafluoroethylene. Part 1: The sulfates and fluorides of Al, Zn, Cu, Ni, Co, Fe and Mn.

G.J. Puts and P.L. Crouse

Department of Chemical Engineering, University of Pretoria, Pretoria 0002, South Africa.

Telephone number of corresponding author: +27 12 420 2670

Email address of corresponding author: Gerard.Puts.UP@gmail.com

ABSTRACT:

The thermal decomposition of PTFE intimately mixed with the solid sulfates and fluorides of selected metals ($\text{Al}_2(\text{SO}_4)_3$, ZnSO_4 , CuSO_4 , NiSO_4 , CoSO_4 , FeSO_4 , AlF_3 , CuF_2 , NiF_2 , CoF_2 , FeF_2 and MnF_2) was investigated by TGA-FTIR. It was found that the sulfates affect the rate of pyrolysis with CuSO_4 lowering mass-loss onset temperature by 60 °C. The fluorides have no effect on the pyrolysis rate, with the exception of AlF_3 which lowers the onset temperature by 35 °C. It was also found that $\text{Al}_2(\text{SO}_4)_3$ and NiSO_4 moderately increase the yield of hexafluoropropylene, and that AlF_3 shifts the product composition to almost exclusively hexafluoropropylene and hexafluoroethane.

KEYWORDS: PTFE pyrolysis; PTFE thermal degradation; filled PTFE, catalytic pyrolysis, TGA-FTIR

1 Introduction

Polytetrafluoroethylene (PTFE) is the world's most used fluoropolymer, accounting for 44% of the fluoropolymers market (29 000 metric tons) in 2008 with an estimated global trade value of 367 million US Dollars [1]. There are four types of PTFE resins commercially available, *viz.* granular, fine powder, dispersions, and micronized powder. Granular PTFE is prepared by suspension polymerisation, while fine- & micronized powders as well as dispersions are mostly prepared *via* emulsion polymerisation. Granular PTFE constitutes the bulk of the PTFE market, accounting for some 45 % of PTFE production in 2008 [1].

Suspension polymerisation produces predominantly high-molecular-weight PTFE. The emulsion process can be tuned to produce a wide range of molecular weights. Emulsion polymerisation requires the use of perfluorinated surfactants, the most common of which is perfluorooctanoic acid (PFOA). PFOA has been shown to impact the environment negatively and is being phased out [1].

A market report from 2009 on the trends in the fluoropolymer industry indicated that the market share of high-molecular-weight PTFE is set to increase due to the phasing out of PFOA [1].

Unlike most other high-polymers, high-molecular-weight PTFE cannot be melt processed [1, 2] and its products are prepared predominantly by mechanical working of a pressed and sintered preform, during which a considerable amount of waste material is produced. The mass of waste generated can account for as much as 50% of the final mass on products of complex geometries [3]. Consequently, PTFE waste cannot be reprocessed *via* the usual methods employed for plastics recycling and presents both an economic loss as well as an ecological problem.

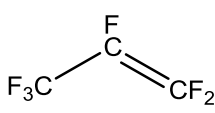
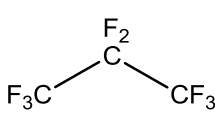
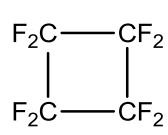
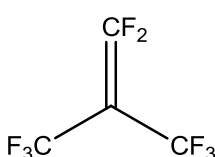
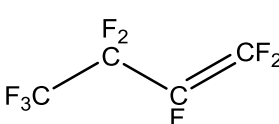
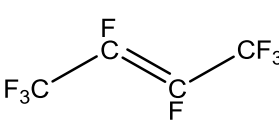
The literature indicates that PTFE may be chemically recycled by pyrolysis to produce mixtures of various high-value chemicals [4]. Much work has been done on the topic of PTFE pyrolysis. The reader is referred to the primary literature and the authors' review for further details [4-30]. Table 1 summarises the species commonly found in the pyrolysis gas of PTFE.

Tetrafluoroethylene (TFE), hexafluoropropylene (HFP), and octafluorocyclobutane (OFCB) are important commercial compounds, with TFE being the monomer from which PTFE is made, while HFP is used as a comonomer for producing polymers such as FEP and Viton [31]. OFCB is primarily used as an etch gas in the electronics industry. OFCB is of special importance in this role as it preferentially etches SiO_2 [32].

Octafluoroisobutene is highly toxic, mainly causing pulmonary oedema, but can also affect the heart muscle [33]. Octafluoro-1-butene and octafluoro-2-butene are not toxic, but are undesirable byproducts as have very limited application in fire fighting [34].

Hexafluoroethane (HFE) and octafluoropropane (OFP) are also undesirable by products as they have very limited application.

Table 1: The names and structures of perfluorinated species commonly found in PTFE pyrolysis gas.

Chemical Name	Abbreviation	Molecular Structure	CAS No:
Tetrafluoroethylene	TFE	$F_2C=CF_2$	116-14-3
Hexafluoroethane	HFE	F_3C-CF_3	76-16-4
Hexafluoropropylene	HFP		116-15-4
Octafluoropropane	OFP		76-19-7
Octafluorocyclobutane	OFCB		115-25-3
Octafluoroisobutene	OFIB		382-21-8
Octafluoro-1-butene	OF1B		357-26-6
Octafluoro-2-butene	OF2B		360-89-4

The literature reveals that the yields of the various species are strong functions of temperature and pressure, and attempts to optimise the yields of the commercially interesting species have focused on control of these parameters. Table 2 summarises the reported product distributions as a function of temperature and pressure. It should be noted here that there is a distinct lack of correlation amongst the data sets presented in the literature.

Table 2: Distribution of products obtained from the pyrolysis of PTFE as function of temperature and pressure.

<u>101325 Pa</u>*						
Temperature (°C)	TFE	HFP	OFCB	OFIB	Perfluorocarbons	Ref.
600	15.9 %	25.7 %	54.3 %	4.1 %	-	[19]
<u>83600 Pa</u>*						
Temperature (°C)	TFE	HFP	OFCB	OFIB	Perfluorocarbons	Ref.
600	32 %	26 %	42 %	-	-	[9]
700	52 %	24 %	18 %	5 %	-	[9]
<u>30000 Pa</u>*†						
Temperature (°C)	TFE	HFP	OFCB	OFIB	Perfluorocarbons	Ref.
600	30.79 %	30.22 %	6.89 %	-	32.1 %	[29]
700	12.17 %	28.32 %	3.76 %	15.47 %	40.28 %	[29]
800	1.17 %	40.60 %	-	6.93 %	51.3 %	[29]
<u>5500 Pa</u>*						
Temperature (°C)	TFE	HFP	OFCB	OFIB	Perfluorocarbons	Ref.
600	85.7 %	14.3 %	<4 %	-	-	[19]
700	82.1 %	17.9 %	<4 %	-	-	[19]
<u>670 Pa</u>*						
Temperature (°C)	TFE	HFP	OFCB	OFIB	Perfluorocarbons	Ref.
500	96.8 %	2.9 %	-	-	-	[21]
600	97 %	3 %	-	-	-	[19]

*Absolute pressure

†In an atmosphere of nitrogen.

As indicated by Table 2, even under optimum conditions, individual species cannot be exclusively produced. The product stream is always a mixture of compounds and must be separated by way of cryogenic distillation. The potential generation of toxic products also forces the requirement that the pyrolysis process operates at conditions that place limits on process scale-up and throughput. The reluctance of commercial entities to engage in pyrolysis recycling of PTFE suggests that this process is not economically feasible at present.

It would be of economic interest if methods could be found to beneficiate PTFE waste catalytically in order to increase selectively the yields of commercially important products in excess of what is possible at present, or eliminate the toxic products by catalytic reformation. These methods would also have application in the wider fluorochemical industry.

There are a few reports in the open literature regarding the catalysed pyrolysis of PTFE or the catalytic reformation of TFE to other perfluorinated compounds. Choi and Park [9] reported a large increase in the yield of TFE (76 to 90%) at 700 °C and 1 bar when using copper instead of Inconel as reactor tube material. Filatov [13] pyrolysed PTFE intimately mixed with CoF_3 in a batch reactor and found that the yields of gaseous products were greatly reduced, but that the yield of perfluoroparaffins (6 to 26 carbons in length) was greatly improved. Fock [5] found that the carbon black used in carbon-filled PTFE contained large numbers of unpaired electrons and that this composite material showed vastly different decomposition rates to neat and bronze-filled PTFE. He also found that the bronze-filled PTFE did not degrade much differently compared with neat PTFE. Finally, Odochian [25] studied glass-, carbon-, and bronze-filled PTFE and found that these filler materials had no significant effect on the degradation rate or the gaseous-product distribution.

The cited literature indicates that work has, up to the present, focused only on potential catalytic effects of filler materials commonly used in the plastics industry. There clearly is a

significant gap in the literature regarding the effects of inorganic materials on the PTFE pyrolysis process.

The pyrolysis of CHF_2Cl (R22) over fluorinated-metal catalysts, studied by Sung and co-workers [35], indicates that fourth period metals and their fluorinated compounds increase conversion of R22 but shift the product distribution from TFE toward partially-fluorinated compounds such as CH_2F_2 , CHF_3 and $\text{F}_2\text{C}=\text{CHF}$. Guided by this result, this paper undertakes, as the first step in developing a catalytic pyrolysis process, to investigate the effects that simple inorganic compounds of the fourth period metals have on the PTFE degradation rate and gaseous product distribution. The present work is the first in a series relating our preliminary results, with this particular communication documenting the effect of the sulphides and fluorides of Al, Zn, Cu, Ni, Co, Fe and Mn, as studied by TGA-FTIR.

2 Results and Discussion

2.1 Generation of IR reference spectra for the product gases

Infrared spectra for simple fluorinated compounds such as CF_4 , TFE, HFE and OFCB are available from NIST [36], but no literature could be found concerning the infrared spectra for HFP, OFP or the octafluorobutenes. Infrared absorption spectra were, therefore, generated for all the expected product species using DFT (B3LYP) with the 6-31+G*, 6-311G* and 6-311++G** basis sets. The DFT (B3LYP) functional has been shown to predict accurately the absorption spectra for both small unsaturated fluorocarbons as well as small to medium saturated fluorocarbons [37]. It was found that the 6-311G* basis set predicted absorption frequencies closest to the available experimental values.

Table 3 compares the calculated absorption frequencies to the experimental frequencies for TFE, HFE and OFCB. Table 4 presents the calculated absorption frequencies for HFP, OFIB, OF1B and the isomers of OF2B.

Table 3: Experimental and predicted IR absorption frequencies for TFE, HFE and OFCB.

Compound	$\nu_{\text{Calculated}}$ (cm^{-1})	$\nu_{\text{Experimental [36]}}$ (cm^{-1})
TFE	1324	1324
	1180	1170
HFE	1230	1248
	1107	1114
OFCB	1322	1337
	1275	1286
	1224	1236
	963	960
	565	570

Table 4: Predicted IR absorption frequencies for HFP, OFIB, OF1B, cis-OF2B and trans-OF2B.

$\nu_{\text{Calculated}} \text{ (cm}^{-1}\text{)}$				
HFP	OF1B	Cis-OF2B	Trans-OF2B	OFIB
1831	1825	1771	1264	1772
1386	1364	1347	1240	1382
1323	1328	1327	1201	1305
1207	1308	1252	1173	1264
1194	1221	1202	883	1231
1155	1215	1166	680	1190
1033	1192	1102		1047
762	1162	954		990
654	1098	717		718
	946			

These infrared absorption frequencies were used to identify the various components present in the pyrolysis product stream.

2.2 Thermal behaviour of pure PTFE

In order to validate the experimental setup and provide a baseline for the filled PTFE experiments, control experiments were carried out using pure PTFE.

The thermograms for these experiments, presented in Figure 1, indicate an onset temperature of around 560 °C, in good agreement with the literature. The temperature derivative of the mass loss curves of Figure 1 are shown in Figure 2. From the derivatives the temperature at which mass loss is first noted was found to be around 450 °C

The degradation also proceeds fairly rapidly, with total decomposition taking approximately 9 minutes and no residue remaining in the crucible afterward.

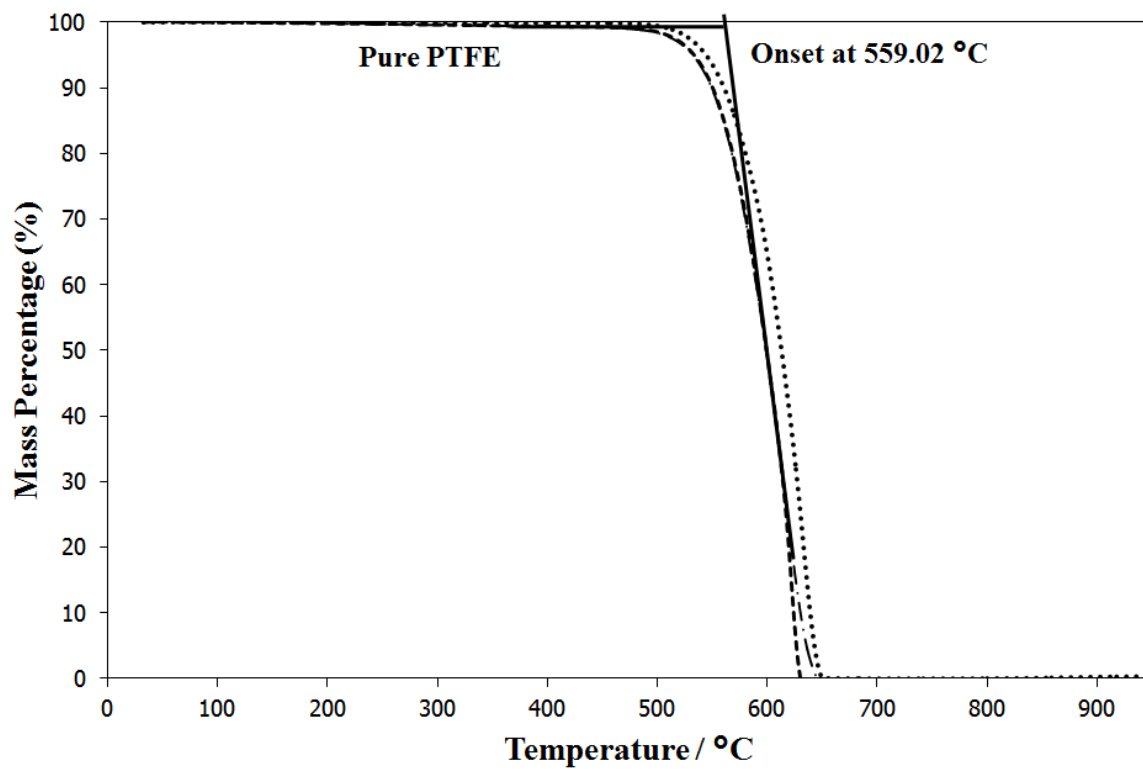


Figure 1: Thermograms for the PTFE control experiments.

Legend for Figure 1

— · - Pure PTFE Run 1

--- Pure PTFE Run 2

..... Pure PTFE Run 3

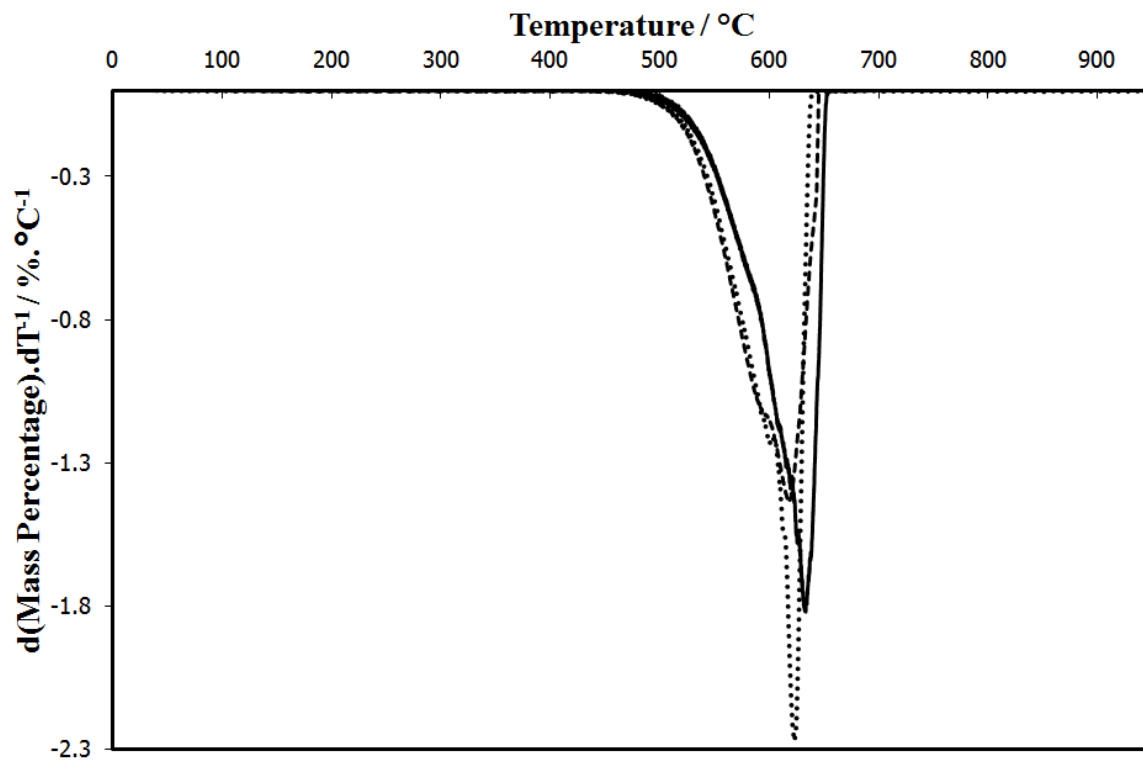


Figure 2: The temperature derivatives plotted against temperature of the pure PTFE thermograms.

Legend for Figure 2

--- Pure PTFE Run 1

— Pure PTFE Run 2

..... Pure PTFE Run 3

The IR spectra for the gas phase were the same for all the control runs, one of which is reproduced in Figure 3. The large bands 1325 cm^{-1} and 1183 cm^{-1} indicate the presence of TFE while those at 1787 cm^{-1} , 1387 cm^{-1} and 1033 cm^{-1} indicate that trace quantities of HFP are also present.

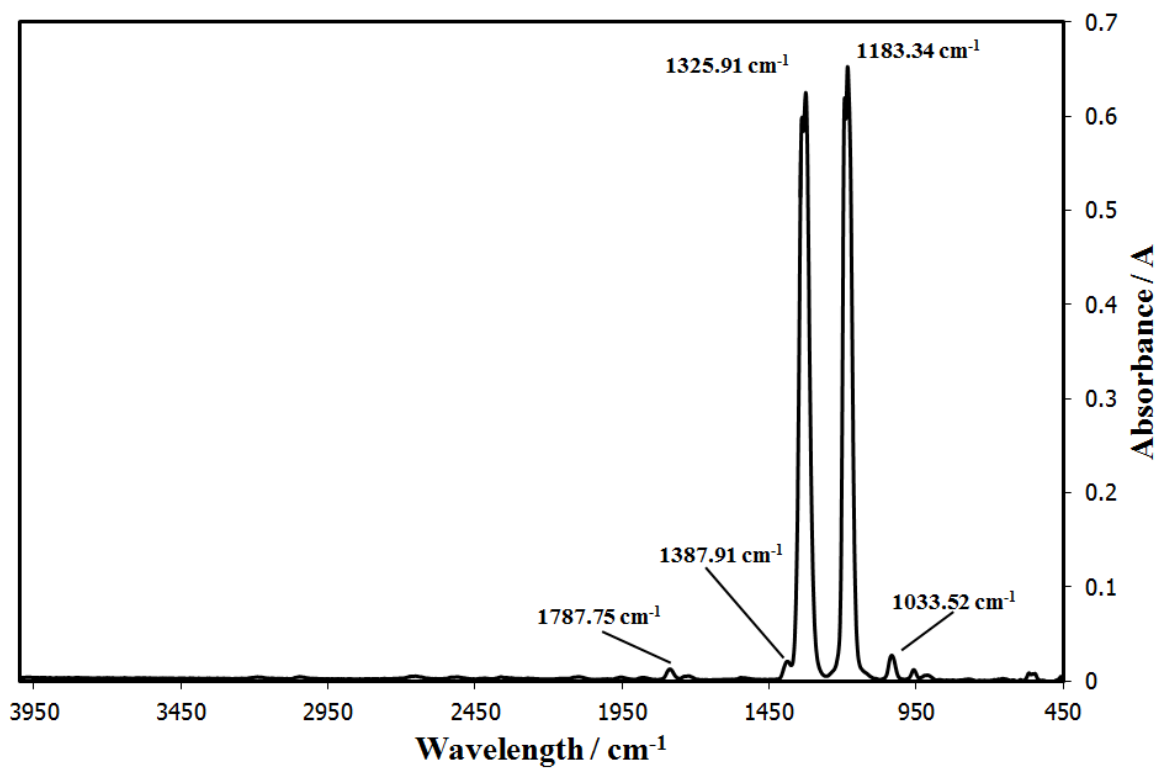


Figure 3: IR Spectrum of the gas phase at maximum absorbance during pyrolysis of pure PTFE.

The gas-phase composition determined for the control experiments are in agreement with those reported by Odochian [25] and Madorski [21]. Keeping in mind that the atmospheric pressure in the laboratory was in the region of 86 kPaa, these results differ strongly with the values reported by Choi and Park [9] (see Table 1), according to whom, nearly equal amounts of TFE and HFP should be observed.

From this we may state that any fluorocarbon species other than TFE noted in the gas phase is produced by chemical interaction of the PTFE pyrolysates with the filler material.

2.3 Thermal behaviour of the neat filler materials

Given the relatively high decomposition temperature of PTFE, potential decomposition of the filler material must be considered when interpreting the results of the filled PTFE experiments.

The literature [38] indicates that $\text{Al}_2(\text{SO}_4)_3$ starts to decompose at 770 °C, ZnSO_4 at 680 °C, CuSO_4 at 650 °C, NiSO_4 at 848 °C, CoSO_4 at 735 °C and FeSO_4 at 480 °C. MnSO_4 melts at 700 °C and decomposes at 850 °C.

AlF_3 sublimates at 1272 °C [39], ZnF_2 melts at 872 °C [38], CuF_2 decomposes at 950 °C, NiF_2 sublimates at 1000 °C, CoF_2 melts at 1200 °C, FeF_2 melts at 1000 °C and MnF_2 melts at 856 °C.

The metal fluorides and metal oxides, in general, exhibit sharp decomposition or sublimation steps with minimal dissociation at temperatures below their melting or sublimation points, but it is understood that the sulfates have no sharp decomposition point and that near to the reported decomposition temperatures they already exhibit a significant degree of dissociation [40].

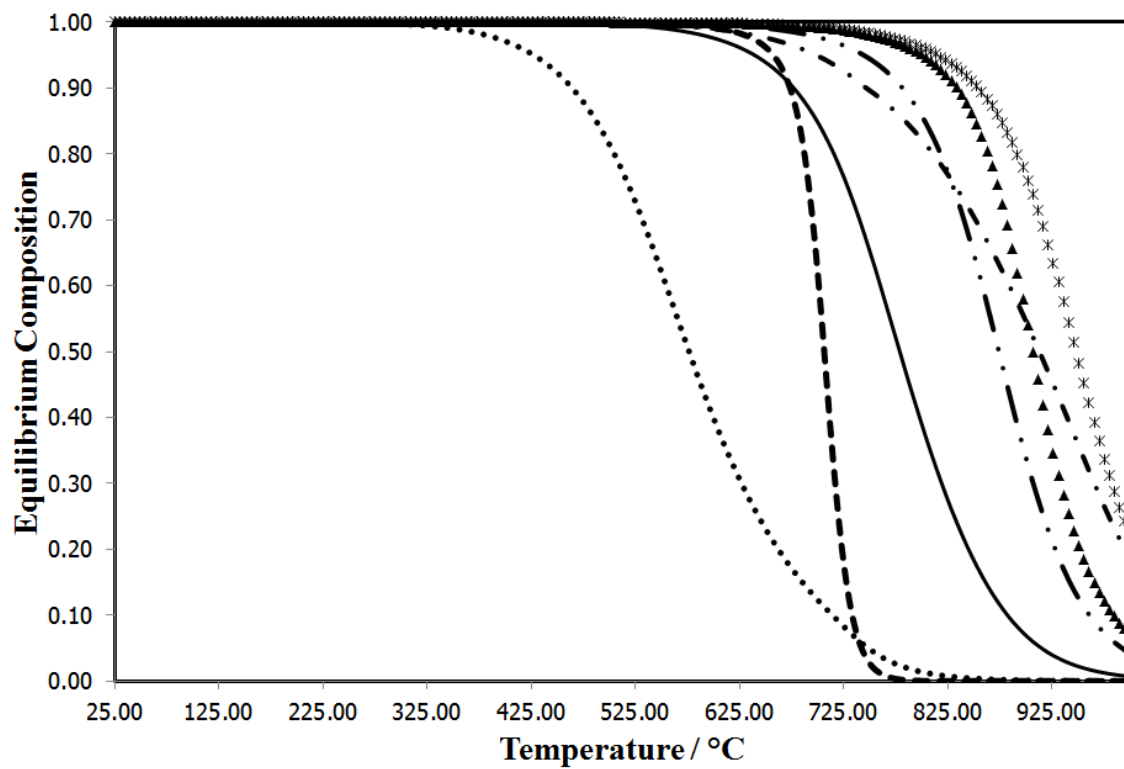


Figure 4: Thermodynamic equilibrium composition of the solid sulfates as a function of temperature.

Legend for Figure 4.

— — $\text{Al}_2(\text{SO}_4)_3$

— · ZnSO_4

—— CuSO_4

—— NiSO_4

* CoSO_4

•••• FeSO_4

▲ MnSO_4

Thermodynamic-equilibrium composition curves for the solid sulfates are presented in Figure 4. The graph indicates that all the sulfates except for FeSO_4 and CuSO_4 should be fully solid during the pyrolysis reaction and, except for the two aforementioned materials, any interactions taking place will be between solid filler and the pyrolysates.

2.4 Thermal behaviour of PTFE filled with transition metal sulfates

The thermograms for the pyrolysis of the sulfate filled PTFE samples are presented in Figures 5 and 6, while the infrared spectra of the gas phase, taken at the point of maximum absorbance, are presented in overlaid format in Figures 7 and 8.

With the exception of CuSO_4 and FeSO_4 filled samples, the onset of degradation temperature does not differ much from that of pure PTFE, varying from $550\text{ }^\circ\text{C}$ to $560\text{ }^\circ\text{C}$. The shapes of the degradation curves at the point of PTFE breakdown do not differ significantly from the control case either, implying that these sulfates do not affect the actual degradation process.

The other significant events present on these curves are the dehydration steps for $\text{Al}_2(\text{SO}_4)_3$, ZnSO_4 , CuSO_4 , CoSO_4 and MnSO_4 , which all occur below $400\text{ }^\circ\text{C}$, as well as the bulk breakdown steps for the sulfates themselves, which occur well past the breakdown of PTFE.

ZnSO_4 and MnSO_4 have no effect on the gas phase, as evidenced by the lack any absorption peaks other than what should be observed for pure PTFE breakdown.

The $\text{Al}_2(\text{SO}_4)_3$ filled samples show TFE as well as additional peaks at 1386 cm^{-1} , 1280 cm^{-1} , 1244 cm^{-1} and 1034 cm^{-1} , with a small shoulder at 1114 cm^{-1} . Absorption at 1244 cm^{-1} and 1114 cm^{-1} indicate the presence of HFE, while the remaining correspond to HFP.

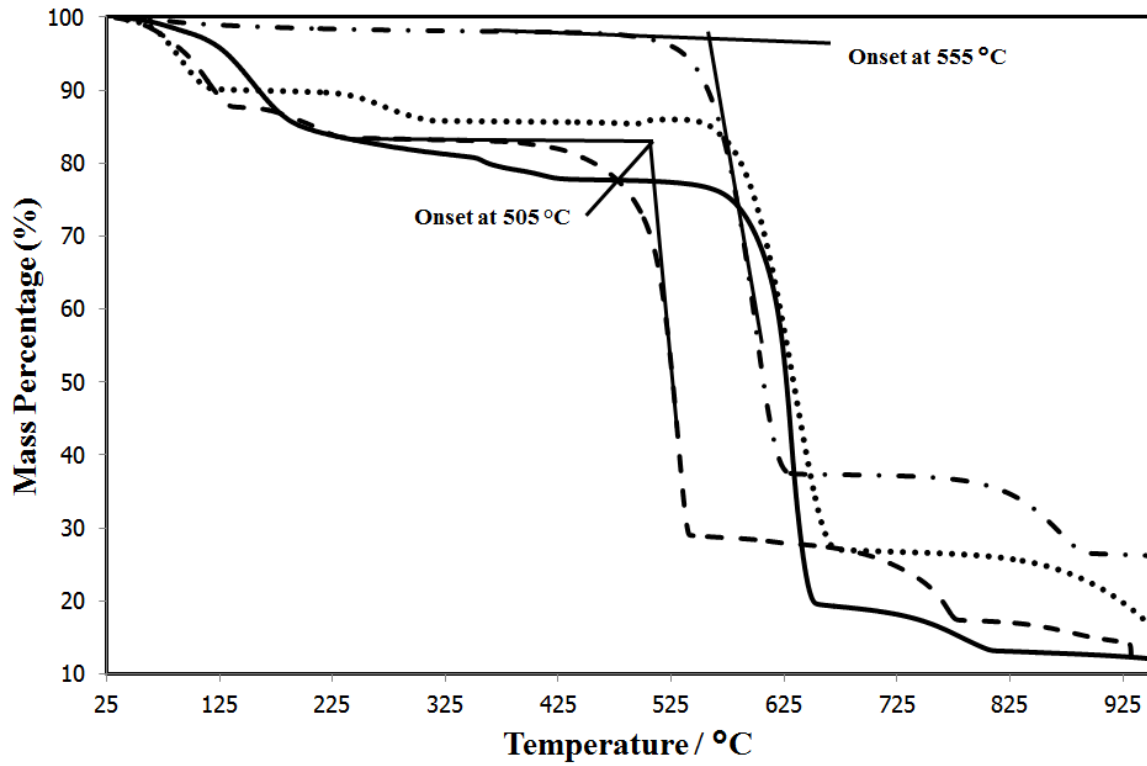


Figure 5: Thermograms for the decomposition of PTFE filled with $\text{Al}_2(\text{SO}_4)_3$, ZnSO_4 , CuSO_4 and NiSO_4 .

Legend for Figure 5.

— $\text{Al}_2(\text{SO}_4)_3$

.... ZnSO_4

- - CuSO_4

- · NiSO_4

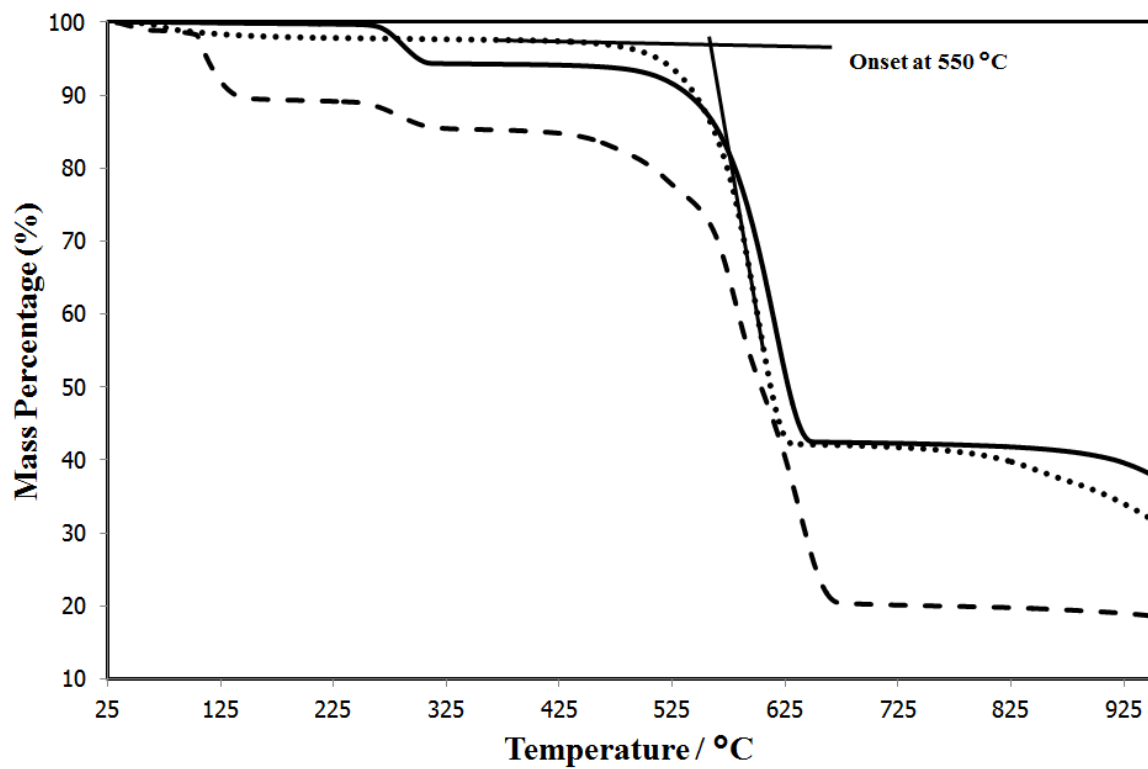


Figure 6: Thermograms for the decomposition of PTFE filled with CoSO_4 , FeSO_4 and MnSO_4 .

Legend for Figure 6.

..... CoSO_4

- - FeSO_4

— MnSO_4

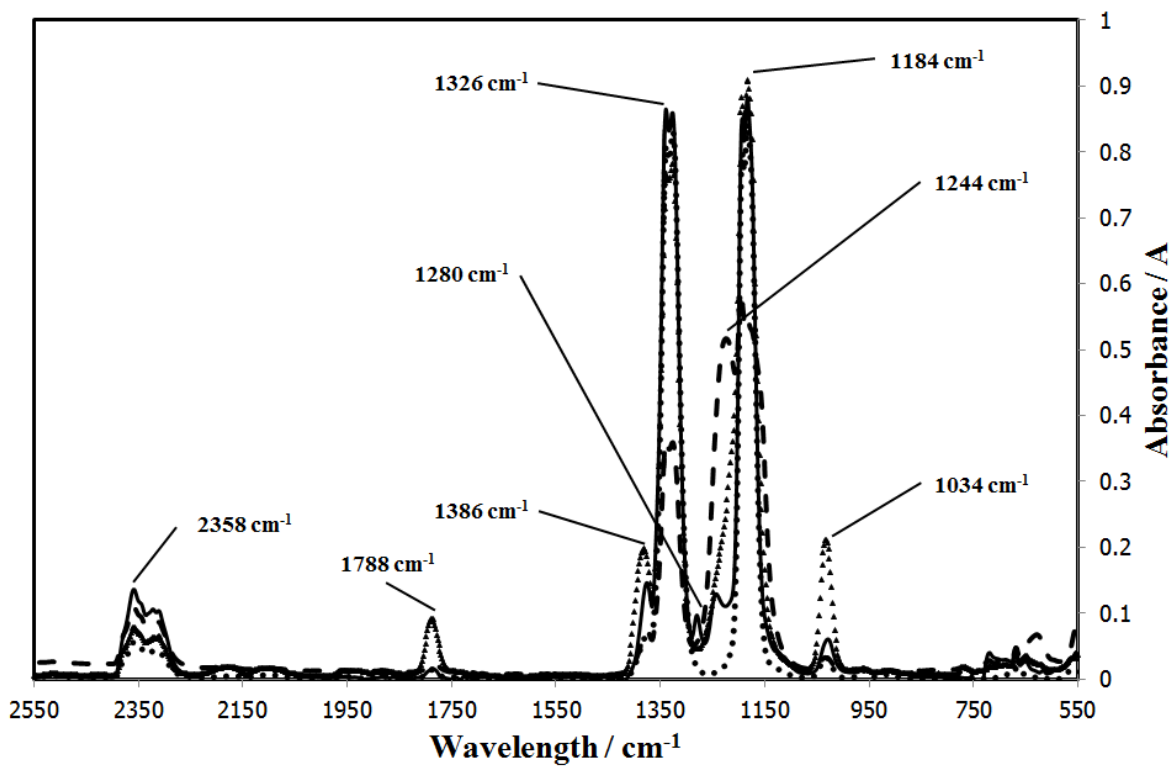


Figure 7: Infrared spectra of the gas phase, taken at the point of maximum absorbance, for the decomposition of PTFE filled with $\text{Al}_2(\text{SO}_4)_3$, ZnSO_4 , CuSO_4 and NiSO_4 .

Legend for Figure 7.

— $\text{Al}_2(\text{SO}_4)_3$

.... ZnSO_4

- - CuSO_4

▲ NiSO_4

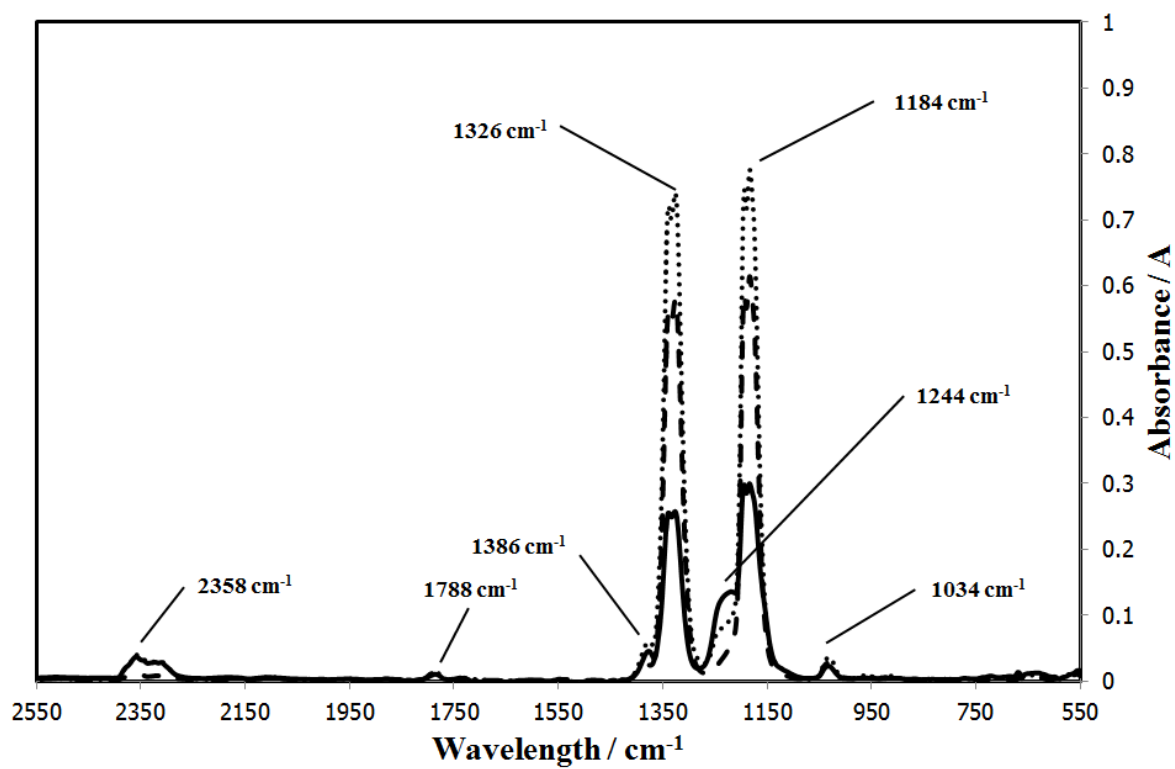


Figure 8: Infrared spectra of the gas phase, taken at the point of maximum absorbance, for the decomposition of PTFE filled with CoSO_4 , FeSO_4 and MnSO_4 .

Legend for Figure 8.

— CoSO₄

..... FeSO₄

- - MnSO₄

The CuSO₄-filled PTFE samples show peaks for TFE as well as a single side peak at 1244 cm⁻¹. Additionally, there are also peaks at the 600 cm⁻¹ and 550 cm⁻¹ mark, attributed to the presence of SO₃.

FeSO₄ and CoSO₄ also produce the side peak at 1244 cm⁻¹. This does not correspond to any of the expected pyrolysis products, and, for the moment, remains unassigned. It was noticed that runs with CuSO₄, FeSO₄ and CoSO₄ produced waxy residues on the inlet of the transfer line with CuSO₄ and CoSO₄ producing the most significant deposits.

The NiSO₄ filled PTFE samples show peaks for TFE as well as side peaks that correspond to the presence of HFP.

All the IR spectra show the presence of CO₂, as indicated by its characteristic absorption band at 2358 cm⁻¹ [36]. The production of CO₂ is attributed to a reaction between the pyrolysates and the oxygen atoms at the surface of the sulfate particles. As the filler residues have not been studied, no conclusion can be drawn regarding the fate of the fluorine atoms which are exchanged during this reaction. However, the presence of side bands would indicate that the fluorine atoms are given to other fluorocarbon species, rather than to the filler material.

Additionally, sooty deposits were noticed in the Al₂(SO₄)₃ residues. Given that PTFE consists of repeating CF₂ units, the production of saturated fluorocarbons requires fluorine exchange reactions between unsaturated fluorocarbon species to produce perfluorocarbons and C_(s). The presence of elemental carbon in the form of soot indicates that this type of exchange has occurred and the production of HFE is thus accounted for.

2.5 Thermal behaviour of transition metal fluoride filled PTFE

The thermograms for the pyrolysis of the fluoride-filled PTFE samples are presented in Figure 9, while the infrared spectra of the gas phase, taken at the point of maximum absorbance, are presented in Figures 10 and 11.

Except for AlF_3 , the onset of degradation temperature is nearly the same for all samples and very close to that of pure PTFE, varying from $565\text{ }^\circ\text{C}$ for CoF_2 to $550\text{ }^\circ\text{C}$ for CuF_2 . Again, except for AlF_3 , the slopes of the degradation curves are all similar to the control case. This indicates that these filler materials have no effect on the degradation process.

The AlF_3 filled PTFE show an onset temperature of $530\text{ }^\circ\text{C}$ as well as a more rapid degradation rate, as evidenced by the steeper slope of the degradation curve.

Observing the gas phase for the transition metal fluorides, we notice that, in addition to the TFE peaks, there is also some shoulder formation in the region of 1244 cm^{-1} . An interesting trend is exhibited in that NiF_2 produces a large shoulder while the shoulder peaks for the other fluorides are quite muted. This continues the trend seen with the sulfates: Nickel compounds have some special interaction with the pyrolysates.

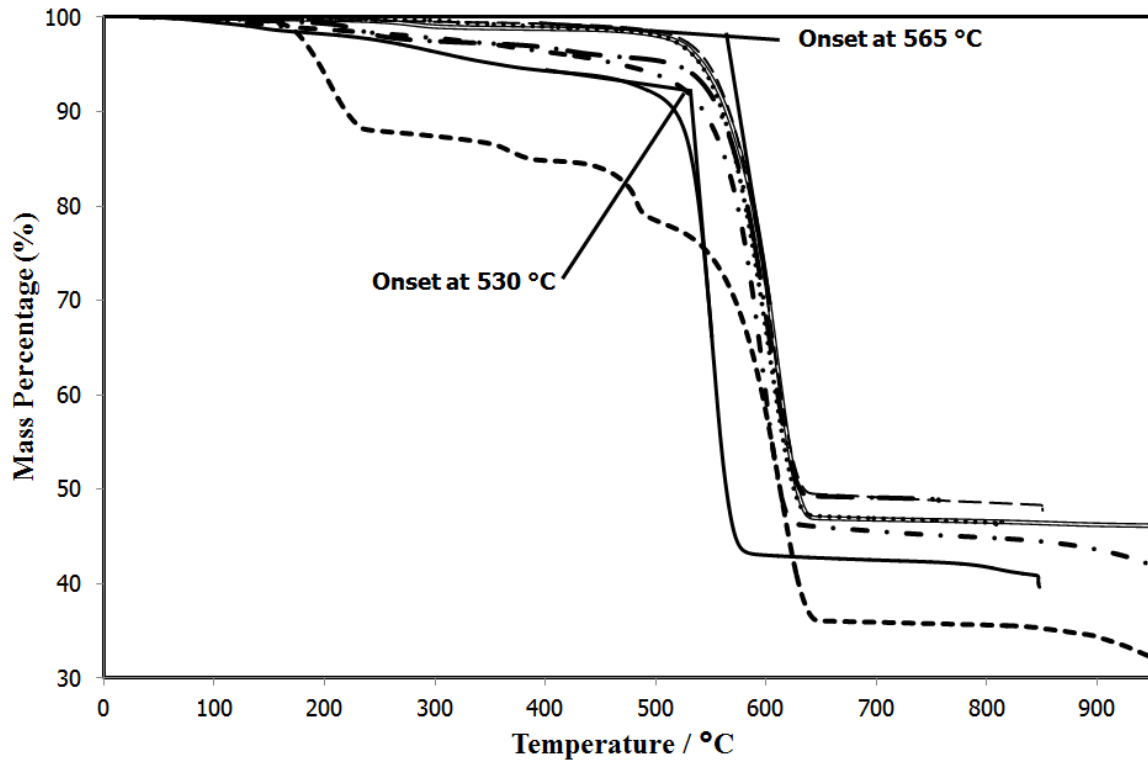


Figure 9: Thermograms for the decomposition of PTFE filled with AlF_3 , ZnF_2 , CuF_2 , NiF_2 , CoF_2 , FeF_2 and MnF_2 .

Legend for Figure 9.

— AlF_3

..... ZnF_2

- - - CuF_2

- . NiF_2

- - CoF_2

— FeF_2

— MnF_2

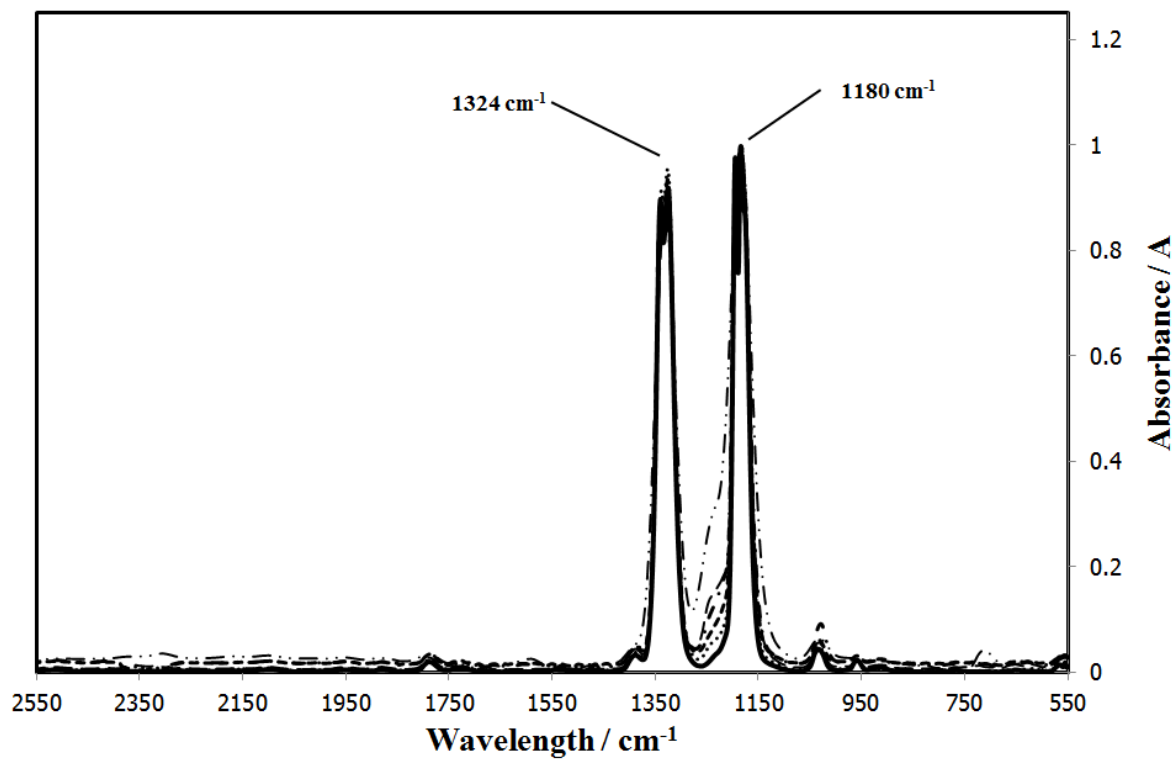


Figure 10: The infrared spectra of the gas phase, taken at the point of maximum absorbance, for the decomposition of PTFE filled with ZnF₂, CuF₂, NiF₂, CoF₂, FeF₂ and MnF₂.

Legend for Figure 10.

— ZnF₂

--- CuF₂

- . . NiF₂

- - CoF₂

..... FeF₂

- . . MnF₂

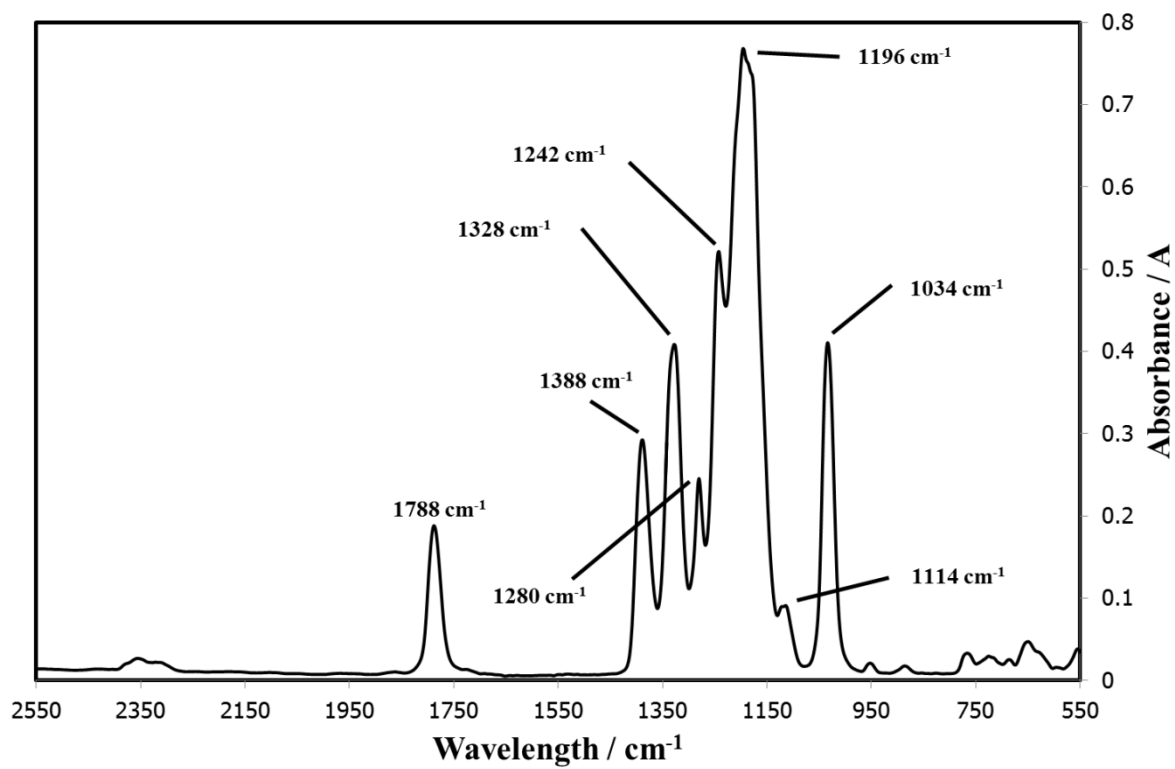


Figure 11: The infrared spectrum of the gas phase, taken at the point of maximum absorbance, for the decomposition of AlF₃-filled PTFE.

The peaks present in the spectrum for the AlF_3 filled PTFE do not correspond to any one known pyrolysis product. Assuming that the gas phase is a mixture of compounds rather than comprised of a new, unexpected species, the peaks at 1114 cm^{-1} and 1242 cm^{-1} indicate the presence of HFE. This assignment is confirmed by the presence of sooty deposits in the AlF_3 residue. The remaining peaks then correspond to HFP. Notably absent are the characteristic peaks for TFE, indicating that AlF_3 almost totally reforms the gas phase to HFP.

The surface of the AlF_3 α -phase (the thermodynamically most stable phase) predominantly exposes the (011 2) plane. Calculations concerning the surface structure showed that this surface is terminated by alternating 6-fold and 5-fold coordinated aluminium ions. The under coordinated aluminium ions are what gives rise to the Lewis acid sites on α -phase AlF_3 [41].

The mechanism of PTFE degradation involves chain scission to produce $:\text{CF}_2$ units which then undergo recombination. The $:\text{CF}_2$ recombination products undergo various radical intermediated reactions that produce the products recovered during PTFE pyrolysis [30]. AlF_3 could arguably capture the difluorocarbenes via attachment of the non-bonding electrons in the carbenes to the open Al sites, thereby facilitating the fluorine rearrangement reactions that produce the observed products.

The reactivity of Co^{2+} and Cu^{2+} is explained by the presence of an unpaired electron in the valence shell which can capture the fluorocarbon radical species generated during pyrolysis. Until the species causing the shouldering at 1244 cm^{-1} is identified, no comment can be made on the possible mechanism by which Co and Cu intermediated catalysis can occur.

3 Conclusions

We have demonstrated that the sulfates of Al, Zn, Ni, Co, Fe and Mn are generally inert with respect to the rate of degradation of PTFE, but that CuSO_4 accelerates the degradation rate and lowers the degradation onset temperature by 50 °C. We have also demonstrated that these compounds all affect the composition of the gaseous product stream with $\text{Al}_2(\text{SO}_4)_3$ and NiSO_4 increasing the yield of HFP.

Furthermore, we have demonstrated that the fluorides of Zn, Cu, Ni, Co, Fe and Mn are generally inert with respect to the rate of degradation of PTFE, but that AlF_3 accelerates the degradation rate and lowers the degradation onset temperature by approximately 30 °C. Finally, we have demonstrated that all these compounds have some effect on the product stream composition, but that AlF_3 displays the strongest effect on the gas phase, seemingly producing exclusively HFE and HFP.

AlF_3 , $\text{Al}_2(\text{SO}_4)_3$ and NiSO_4 show potential as catalysts for the selective beneficiation of PTFE waste by pyrolysis to higher value chemicals.

4 Experimental

4.1 Sample preparation

Analysis grade (purity >99%) $\text{Al}_2(\text{SO}_4)_3$, ZnSO_4 , CuSO_4 , NiSO_4 , CoSO_4 , FeSO_4 and MnSO_4 we purchased from Saarchem and used as received. AlF_3 , ZnF_2 , CuF_2 , NiF_2 , CoF_2 , FeF_2 and MnF_2 (purity >99%) were purchased from Sigma Aldrich and used as received. PTFE 807NX originating from DuPont was used as received.

TGA samples were prepared by grinding 1 g of inorganic material with 1 g of PTFE in a mortar-and-pestle until the mixture appeared macroscopically homogeneous and stored in airtight glass vials. Photographs of $\text{CoSO}_4/\text{PTFE}$ and FeF_2/PTFE mixtures are presented in Figures 12 and 13 to demonstrate the degree of mixedness of the PTFE/inorganic systems.

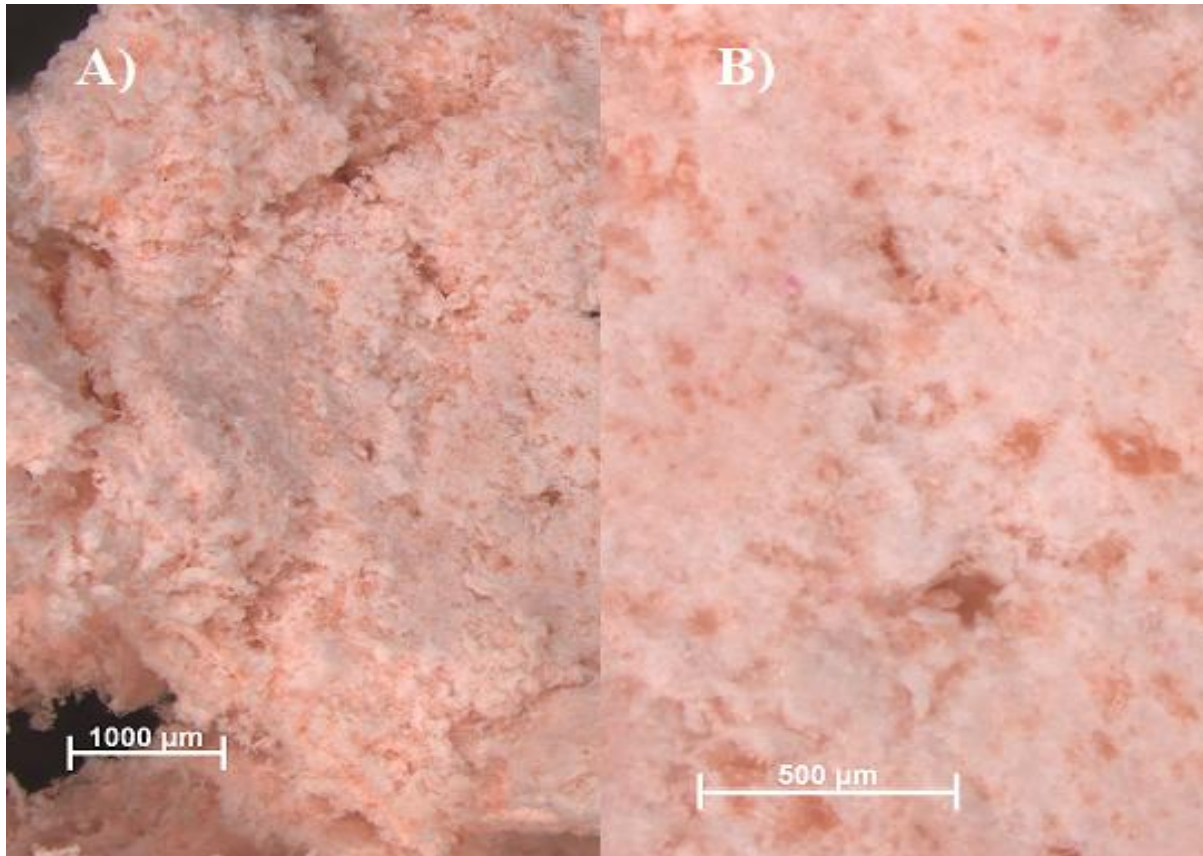


Figure 12: Photographs of the CoSO₄/PTFE mixture at a) 15X magnification and b) 50X magnification.

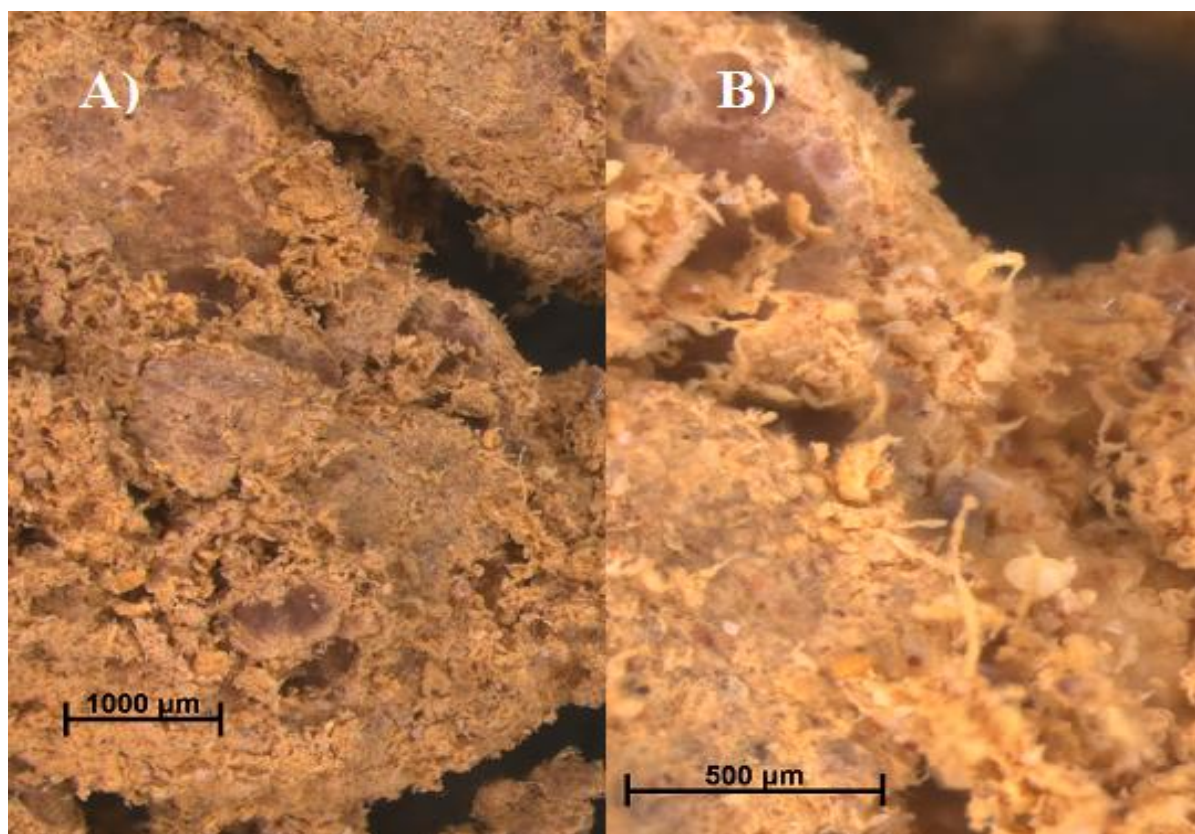


Figure 13: Photographs of the FeF_2/PTFE mixture at a) 15X magnification and b) 50X magnification.

4.2 Quantum chemical & thermodynamic equilibrium calculations

Quantum chemical calculations were performed with the Spartan 06 software suite [42] using DFT (B3LYP). Each molecule was simulated using the 6-31+G*, 6-311G* and 6-311++G** basis sets. The calculations were performed on a desktop computer supplied by Hewlett-Packard equipped with a 3.2 GHz Intel i7 2600 processor and 16 GB of memory.

The thermodynamic equilibrium composition calculations were performed using Outotec's HSC 6.1 software suite [43].

4.3 TGA-FTIR analysis

TGA-FTIR experiments were conducted by placing approximately 50 mg of PTFE/filler mixture in α -alumina crucibles and pyrolysing it in a PerkinElmer TGA 4000 with the gaseous product transferred *via* a heated line to a PerkinElmer Spectrum 100 equipped with a heated transmission gas cell.

The samples were heated at a rate of 20 °C/min from 35 °C to 950 °C in an atmosphere of nitrogen flowing at 20 mL/min. The sampling port area immediately above the furnace was purged with nitrogen at a rate of 150 mL/min. The heated transfer line and IR gas cell were kept at 225 °C. Transfer of the sample from the TGA to the cell took place at a rate of 40 mL/min, thus diluting the sample with an extra 20 ml/min of nitrogen.

The spectrometer was set to take one scan every 6 s in the range of 4000 cm^{-1} to 550 cm^{-1} at a resolution of 4 cm^{-1} . The gas cell was fitted with KBr windows.

5 Acknowledgements

The authors would like to acknowledge the National Research Foundation of South Africa and the Department of Science and Technology's Fluorochemical Expansion Initiative for financially supporting this research.

References

- [1] T. Hayes, K. Furst, H. Richards, Industry Study 2496: Fluoropolymers, The Freedonia Group, Cleveland, Ohio, 2009.
- [2] C.E. Schildknecht, Vinyl and Related Polymers, John Wiley & Sons, Inc., New York, 1952.
- [3] J.G. Drobny, Technology of Fluoropolymers, CRC Press, Boca Raton, 2000.
- [4] C.M. Simon, W. Kaminsky, Polymer Degradation and Stability, 62 (1998) 1-7.
- [5] J. Fock, Journal of Polymer Science Part B: Polymer Letters, 6 (1968) 127-131.
- [6] B.C. Arkles, R.N. Bonnett, in, Liquid Nitrogen Processing Corporation, United States of America, 1974.
- [7] B.B. Baker Jr, D.J. Kasprzak, Polymer Degradation and Stability, 42 (1993) 181-188.
- [8] P.S. Bhadury, S. Singh, M. Sharma, M. Palit, Journal of Analytical and Applied Pyrolysis, 78 (2007) 288-290.
- [9] J.D. Park, S.K. Choi, Journal of the Korean Chemical Society, 20 (1976) 141-145.
- [10] J.A. Conesa, R. Font, Polymer Engineering & Science, 41 (2001) 2137-2147.
- [11] G.D. Dixon, W.J. Feast, G.J. Knight, R.H. Mobbs, W.K.R. Musgrave, W.W. Wright, European Polymer Journal, 5 (1969) 295-306.
- [12] S.-S. Choi, Y.-K. Kim, Journal of Analytical and Applied Pyrolysis, 92 (2011) 470-476.
- [13] V.Y. Filatov, A.V. Murin, S.A. Kazienkov, S.V. Khitrin, S.L. Fuks, Russ J Appl Chem, 84 (2011) 147-150.
- [14] R.E. Florin, L.A. Wall, D.W. Brown, L.A. Hymo, J.D. Michaelson, Journal of Research of the National Bureau of Standards, 53 (1954) 121-130.
- [15] A.N. García, N. Viciano, R. Font, Journal of Analytical and Applied Pyrolysis, 80 (2007) 85-91.
- [16] R.J. Hunadi, K. Baum, Synthesis, 1982 (1982) 454-454.
- [17] G.J. Knight, W.W. Wright, Journal of Applied Polymer Science, 16 (1972) 739-748.
- [18] S.V. Kotov, G.D. Ivanov, G.K. Kostov, Journal of Fluorine Chemistry, 41 (1988) 293-295.
- [19] E.E. Lewis, M.A. Naylor, Journal of the American Chemical Society, 69 (1947) 1968-1970.
- [20] J. Lonfei, W. Jingling, X. Shuman, Journal of Analytical and Applied Pyrolysis, 10 (1986) 99-106.

- [21] S.L. Madorsky, V.E. Hart, S. Strauss, V.A. Sedlak, *Journal of Research of the National Bureau of Standards*, 51 (1953) 327-333.
- [22] E. Meissner, A. Wróblewska, E. Milchert, *Polymer Degradation and Stability*, 83 (2004) 163-172.
- [23] J.D. Michaelson, L.A. Wall, *Journal of Research of the National Bureau of Standards*, 58 (1957) 327-331.
- [24] S. Morisaki, *Thermochimica Acta*, 25 (1978) 171-183.
- [25] L. Odochian, C. Moldoveanu, A.M. Mocanu, G. Carja, *Thermochimica Acta*, 526 (2011) 205-212.
- [26] E.C. Penski, I.J. Goldfarb, *Journal of Polymer Science Part B: Polymer Letters*, 2 (1964) 55-58.
- [27] J.C. Siegle, L.T. Muus, T.-P. Lin, H.A. Larsen, *Journal of Polymer Science Part A: General Papers*, 2 (1964) 391-404.
- [28] M. Tamayama, T.N. Andersen, H. Eyring, *Proceedings of the National Academy of Sciences*, 57 (1967) 554-561.
- [29] I.J. van der Walt, A.T. Grunenburg, J.T. Nel, G.G. Maluleke, O.S.L. Bruinsma, *Journal of Applied Polymer Science*, 109 (2008) 264-271.
- [30] G.J. Puts, P.L. Crouse, B. Ameduri, Thermal degradation and pyrolysis of tetrafluorethylene, in: D.W. Smith, S.T. Iacono, S.S. Iver (Eds.) *Handbook of Fluoropolymer Science and Technology*, John Wiley & Sons, Inc., New York, 2014.
- [31] J.P. Carlson, W. Schmiegell, Fluoropolymers, Organic, in: W. Gerhartz (Ed.) *Ullmann's Encyclopedia of Industrial Chemistry*, Wiley-VCH, Weinheim, 2005.
- [32] J.J. Mezzapelle, in, *International Business Machines Corporation*, 2005.
- [33] C.M. Timperley, *Journal of Fluorine Chemistry*, 125 (2004) 685-693.
- [34] D.D. Back, L.R. Grzyll, C. Ramos, N.A. Samad, in, *Google Patents*, 1997.
- [35] D.J. Sung, D.J. Moon, S. Moon, J. Kim, S.-I. Hong, *Applied Catalysis A: General*, 292 (2005) 130-137.
- [36] I. Coblenz Society, *Evaluated Infrared Reference Spectra*, in: P.J. Linstrom, W.G. Mallard (Eds.) *NIST Chemistry WebBook*, NIST Standard Reference Database Number 69, National Institute of Standards and Technology, 2013.
- [37] L.N. Ignat'eva, V.M. Buznik, *Russ. J. Phys. Chem.*, 80 (2006) 1940-1948.
- [38] R.C. Weast, Section B: Elements and Inorganic Compounds, in: *CRC Handbook of Chemistry and Physics* CRC Press, Cleveland, Ohio, 1974.
- [39] J. Aigueperse, P. Mollard, D. Devilliers, M. Chemla, R. Faron, R. Romano, J.P. Cuer, Fluorine Compounds, Inorganic, in: W. Gerhartz (Ed.) *Ullmann's Encyclopedia of Industrial Chemistry*, Wiley-VCH, Weinheim, 2005.
- [40] J. Hammerschmidt, M. Wrobel, in: *The Southern African Institute of Mining and Metallurgy's Sulphur and Sulphuric Acid Conference 2009*, The Southern African Institute of Mining and Metallurgy, Johannesburg, South Africa, 2009.
- [41] C.L. Bailey, S. Mukhopadhyay, A. Wander, B.G. Searle, N.M. Harrison, *The Journal of Physical Chemistry C*, 113 (2009) 4976-4983.
- [42] W. Inc., in, *Wavefunction Inc.*, Irvine, California, United States of America, 2006.
- [43] A. Roine, in, *Outotec Research*, Oy, Pori, Finland, 2008.